ELSEVIER

Thermochimica Acta 325 (1999) 19–24

thermochimica acta

Water of hydration and cross-linking in live and dead cells

M.C. Ramos-Sánchez, J. Martín-Gil, M.T. Barrio-Arredondo, F.J. Martín-Gil*

"INSALUD&University of Valladolid" Research Unit, Hospital Universitario "Del Río Hortega", Avda. Santa Teresa, s/n, 47010 Valladolid, Spain

Received 14 April 1998; received in revised form 26 August 1998; accepted 31 August 1998

Abstract

Thermal analysis has been used successfully for the in vitro estimation of aging-related changes in biological materials, such as human erythrocytes and spermatozoa, human ear cartilage and porcine scleral tissue cells. Through low-temperature DSC curves we have observed that, as a cellular population ages, the glass-transition temperature of the overall cellular constituents ($-31^{\circ}>T_g>-50^{\circ}C$) shifts to higher values. Conversely, the usual procedures followed in cryobiology to improve cellular survival (i.e. procedures that use rapid freezing by vitrification in a sugar medium, like sucrose, glycerol and PPG, to reduce the amount of freezable water in the live cells) shift the T_g to lower temperatures. Thus, T_g has been shown to be a very good marker in the control of the in vitro vitality degree of a cellular population. Statistically, the cellular life-to-death curves, both for erythrocytes and spermatozoa, can be described by a cubic model.

Keywords: Aging; Cross-linking; Cryobiology; Differential scanning calorimetry; Erythrocytes; Spermatozoa; Vitrification

1. Introduction

Considerable research has been undertaken to explain the state of water [1–7] and molecular cross-linking [8,9] in biological systems. Calorimetry is a favoured method for the study of both subjects, given that information in the physical state and properties of water can be deduced through its solidification or vaporization patterns, and that the amount of molecular cross-linking can be obtained from the thermolysis step. There are many ways of putting calorimetry into use. Based on our experience, we have chosen differential scanning calorimetry (DSC) for low temperatures and differential thermal analysis (DTA) for high temperatures.

Under cooling, two types of water can be distinguished: freezable water, which can be solidified into ice, and 'unfreezable' water, whose behaviour is accounted for by the strong interactions with substrates (structural components, solutes and/or insoluble solids). The nature of the interaction between freezable water and substrates is weak.

In biomaterials, it has been observed that sugars, polyols or sodium hydroxide reduce the amount of freezable water and promote plasticization and molecular mobility of substrate molecules [10]. It can, after thawing, even favour their solubilization [11].

In any case, the substrates–water interactions are affected by substrate cross-linking. With ageing, the cross-links between substrate molecules become increasingly thermostable, so that rigidity and insolubility of biological systems increase [12]. Cross-linking agents include glutaraldehyde, N-succinimidyl 4-(N-maleimido)-butylate, sulphides, polyvalent metals and alkylation reagents.

*Corresponding author.

0040-6031/99/$ – see front matter
PII: S0040-6031(98)00543-7

In order to better understand the process of ageing and the optimal conditions to assure in vitro cellular survival, we undertook a study on the variation over time of both, glass transitions at low temperatures and cross-linking transitions at high temperatures in model systems. The model systems studied were erythrocytes (somatic cells), spermatozoa (reproductive non-dividing, non-synthesizing cells) [13], bacterial cells (which do not age), and scleral tissue and human ear cartilage cells (collagen-containing simple systems).

2. Experimental

2.1. Apparatus

DSC and DTA curves were carried out with Perkin–Elmer DSC 7 and DTA 1700 apparatuses, respectively. Potassium concentration in erythrocyte lysates was measured with an Instrumentation Laboratory BGE apparatus. Motility of spermatozoa was measured using a Leitz Laborlux D microscope.

Reported DSC curves were registered in dynamic N_2 (20 cm^3 min^{-1}), at a heating rate of 10°C min^{-1}, and with 40 μl sealed aluminium capsules as sample containers. DTA curves were obtained in dynamic N_2 (20 cm^3 min^{-1}), at a heating rate of 10°C min^{-1}, and with ceramic crucibles containing aluminium oxide. In both, DSC and DTA experiments the amount of sample used was 10 mg.

2.2. Samples and procedures

Motility and DSC studies for spermatozoa were carried out on human ejaculates after collection in clean polystyrene containers. The analyses were delayed until liquefaction (which occurs within 20 min) because spermatozoa attain full motility only after this process is complete.

Specimens for measure of potassium concentration were prepared by centrifuging 8 ml of whole blood from healthy individuals at 1500×g, removing the plasma, and washing the erythrocyte pellet twice with isotonic saline. The erythrocytes were then resuspended in isotonic saline, homogenized and distributed in seven aliquots. These aliquots were stored at 4°C until analysis (at 40, 65, 70, 185 and 285 min). When the time of analysis was reached, each aliquot was centrifuged and the concentration of K^+ in the supernatant measured.

Bacterial cells were obtained as reported elsewhere [14].

Porcine scleral tissue and human ear cartilage samples were not manipulated.

Human samples (erythrocytes, spermatozoa and ear cartilage) were obtained following procedures in accordance with the Helsinki Declaration of 1975, as revised in 1983.

2.3. Statistical analysis

Curvilinear estimation regression analysis was obtained by the SPSS program for MS Windows.

3. Results

3.1. Studies at low temperatures

Fig. 1 shows the low-temperature DSC scans of a pair of live/dead bacterial cell lyophilates. It is observed that the killed cells from *Brucella abortus* RB51 strains induce a thermal effect whose onset temperature (−42.1°C) is higher by 8°C than that of the live cells (−50.4°C). The observation of this different thermal behaviour, which can be extended to other bacterial cells (unpublished results), was our starting point for studies on the in vitro spontaneous death of select human cells and collagen-containing systems.

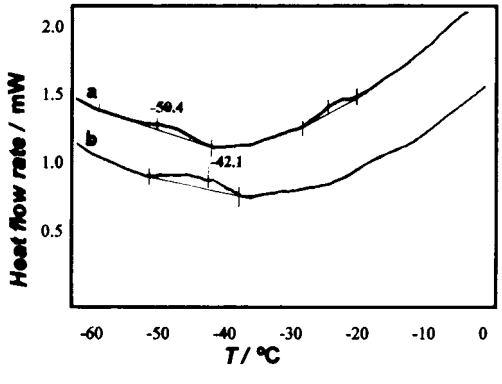

Fig. 1. DSC scans for bacterial cell lyophilates (*Brucella abortus* RB51 strains): (a) live cells; and (b) killed cells.

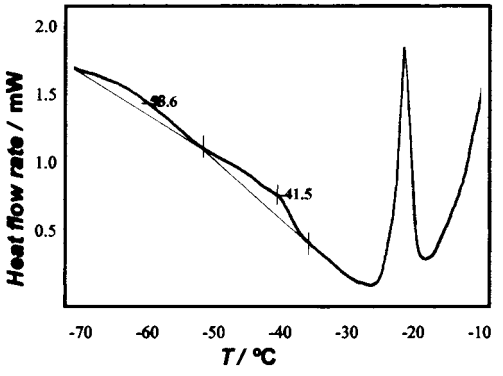

Fig. 2. DSC rewarming curve for human erythrocytes after cooling to −100°C.

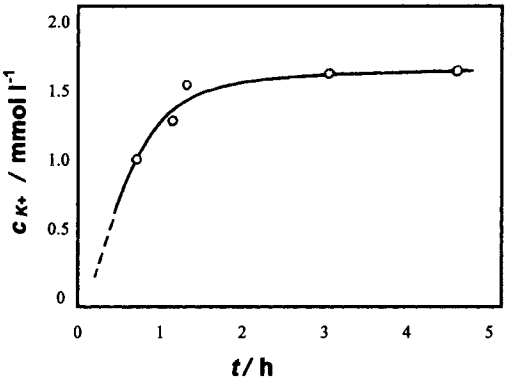

Fig. 4. Effect of the time on the release of a marker as K^+ ions from erythrocytes, measured in a resuspension liquid at room temperature.

In our search for the thermal pathway that leads from life to death, we have studied two sets of selected human cells, namely erythrocytes and spermatozoa.

Fig. 2 shows the DSC rewarming curve for human erythrocytes after cooling to −100°C. The endothermic effects that appear at −60°, −20° and ca. 0°C are independent of erythrocyte vitality but the effect that occurs between −50° and −32°C, attributed to glass transition, shows temperatures (T_g) that vary largely with the time (t) elapsed from venous extraction (Fig. 3). This variation is similar to that of the effect of time on the release of a marker as K^+ ions from cells, measured in a resuspension liquid at room temperature (Fig. 4). Both graphs, Figs. 3 and 4, are curves that follow the cubic model $y=b_0+b_1x+b_2x^2+b_3x^3$, where $b_0=-66.872$, $b_1=17.57$ and $b_2=1.24$ for T_g vs. t; and $b_0=0.0239$, $b_1=1.926$, $b_2=-0.65$ and $b_3=0.066$ for K^+ vs. t. The degrees of fit of the experimental data to these theoretical relationships are $R^2=0.999$, d.f.=1, $F=1016$ and Sigf=0.022 for T_g vs. t; and $R^2=0.989$, d.f.=2, $F=58$ and Sigf=0.017 for K^+ vs. t. In view of the change in slope revealed by the curve in Fig. 3, which occurs at a temperature ca. −34°C, it could be possible to take this temperature to mark the boundaries between domains with different prognostics.

Fig. 5 shows the DSC rewarming curve for human spermatozoa after cooling to −150°C. The DSC trace displays three weak endothermic effects at ca. −80°, −60° and −45°C, followed by a further sharp endothermic peak at ca. 0°C. The endothermic peak observed at ca. −45°C (T_g) shifts to higher temperatures as vitality decreases: four hours after ejaculation, it appears at −41.7°C and two hours later it occurs at

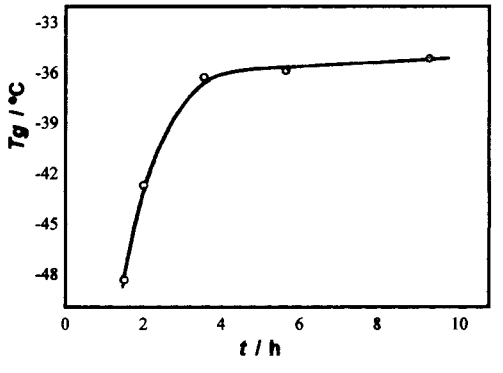

Fig. 3. Effect of the time elapsed from venous extraction on erythrocyte T_g.

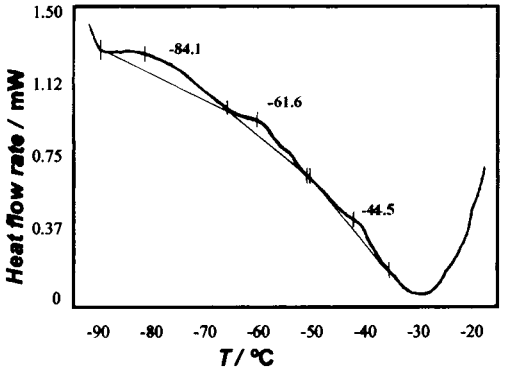

Fig. 5. DSC rewarming curve for human spermatozoa after cooling to −150°C.

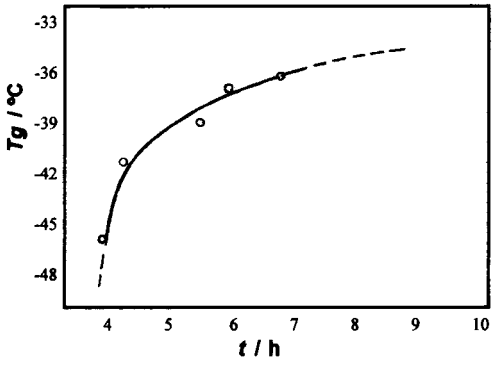

Fig. 6. Effect of the time elapsed from ejaculation on spermatozoa T_g.

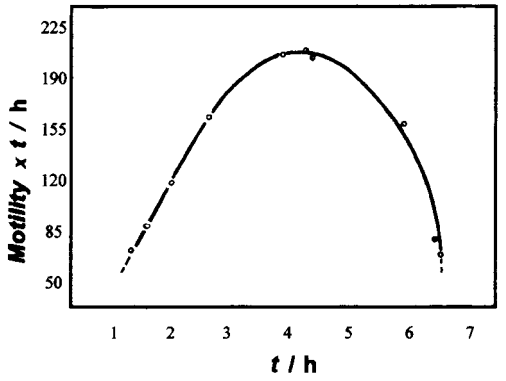

Fig. 8. Effect of the time after ejaculation on the spermatozoa motility×time factor.

−36.7°C (Fig. 6). The critical temperature of the spermatozoa should be −41.5°C, as can be seem from the change in slope shown in Fig. 6. In order to obtain more information on the spermatozoa ageing type, we compared the earlier curve with that resulting from plotting the percentage motility (M) of spermatozoa vs. time after ejaculation (Fig. 7). Both graphs follow the cubic model $y=b_0+b_1x+b_2x^2+b_3x^3$, where $b_0=-96.41$, $b_1=20.02$ and $b_2=-1.555$ for T_g vs. t, and $b_0=91.81$, $b_1=-13.87$, $b_2=2.80$ and $b_3=-0.43$ for M vs. t. The degree of fit of the experimental data to these theoretical relationships gives $R^2=0.800$, d.f.=1, $F=1.99$ and Sigf=0.448 for T_g vs. t; and $R^2=0.998$, d.f.=3, $F=429$ and Sigf=0.001 for M vs. t. On the other hand, given that in a plot of Mt vs. t (Fig. 8) four hours after ejaculation, the product Mt is at a maximum, we can deduce that the temperature associated to this time in Fig. 6 (i.e. −41.5°C) has been appropriately considered critical.

Low-temperature DSC was also applied to study the time-related changes in collagen-containing biological systems, such as the non-cross-linked collagen from porcine scleral tissue (that closely resembles human eye collagen molecules) and human ear cartilage cells (composed of collagen (50%), proteoglucans, water (40%) and chondrocytes). The DSC rewarming curve for porcine eye collagen shows, at ca. −27°C (Fig. 9(a)), the same ageing-related endotherm shown by erythrocytes (at −34°C) and spermatozoa (at −42°C). In addition, this endotherm is present in the DSC curve of a recently-cut human ear sample after cooling to −100°C (Fig. 9(b)): it

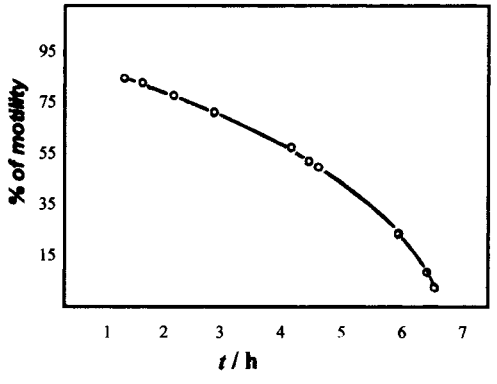

Fig. 7. Effect of the time after ejaculation on the percentage motility of spermatozoa.

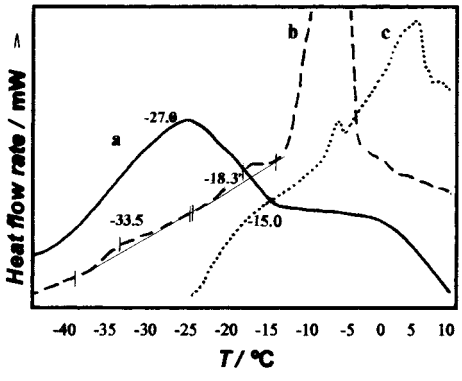

Fig. 9. DSC rewarming curves after cooling to −100°C from: (a) porcine eye collagen; (b) recently-cut human ear sample; and (c) this same sample a day later.

takes place at −33.5°C, followed by two other effects at −18.3° and at ca. 0°C. The DSC curve for this same sample, a day later (Fig. 9(c)), shows a shift of the first of these thermal effects to −15°C (thus, 24 h of ageing and a brief exposure to air resulted in an increase in the glass-transition temperature of nearly 20°C).

So far, all our results coincide in that, whatever the nature and origin of the frozen cellular populations under study, their rewarming curves show a common critical temperature in the −50° to −31°C that shifts to higher temperatures with ageing.

In order to show that alcohols used in cryobiology as preservative agents are effective, collagen gels formed in the presence of methanol and ethylene glycol were frozen and calorimetrically rewarmed. In these conditions, the DSC curves presented slight shifts of T_g to lower temperatures. Also, a similar thermal feature was observed while working with alkaline pH and by conjugation with glucose or xylose.

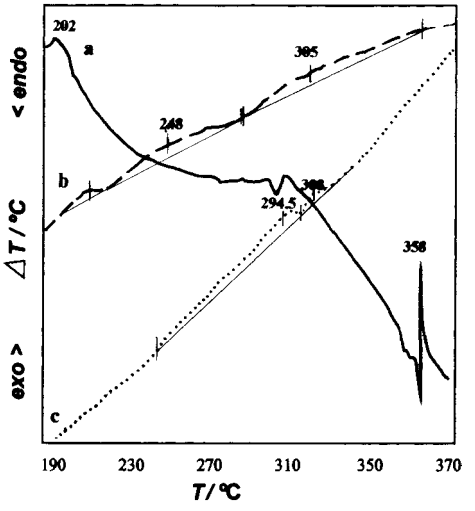

Fig. 10. High-temperature DTA curves for non-aged collagen-containing systems: (a) collagen from porcine scleral tissue; (b) fresh cartilage cells; (c) cartilage cells after a day of ageing and final exposure to air.

3.2. Studies at high temperatures

The high-temperature DTA curves from bacteria, erythrocytes and spermatozoa show variations in their shape according to cellular vitality: whereas only endotherms appeared for live cells, well-defined exotherms were observed for dead cells.

High-temperature DTA curves for non-aged collagen-containing systems showed that collagen exotherms (from porcine scleral tissue) occurred in the 263–290°C range, characteristic of the decomposition of neutral polysaccharides, and at 357.6°C, attributable to decomposition of protein components (Fig. 10(a)). In fresh cartilage cells (Fig. 10(b)), the characteristic carbohydrate component decomposition occurred in the 247–263°C range, while that of the protein components takes place at 305°C. After a day of ageing and final exposure to air, the first peak is shifted to 294.5°C whereas the second peak shifts only to 308.5°C (Fig. 10(c)). These results indicate that cartilage-cell ageing primarily affects stability of the carbohydrate moiety of their various constituents. Thermostability differences seem to confirm the hypothesis that, after dehydration, a stabilization of the macromolecular network occurs in a different way: a stronger association of the glycoprotein–proteoglycan–collagen complexes by cross-linked binding instead of the intramolecular interactions as in the original structure.

4. Discussion

The carefully-controlled low-temperature experimental conditions with erythrocytes and spermatozoa (non-lyofilization, non-delayed study) and the excellent relationship of our results with those obtained from other ageing cellular tests, led us to conclude that:

(i) the glass-transition temperature is an adequate in vitro cellular ageing marker; and
(ii) the temperatures and times that define the first step of the glass temperature-vs.-time curves are the most useful conditions for preventing cellular injury.

Beyond a critical time, the freezing temperature differences among cells in the ageing process are progressively smaller.

At high temperatures, the differences observed in the live and dead cells DSC curves can be explained as being due to both, the existence of different hydration and to the existence of different amount of inter-

molecular and intramolecular cross-links throughout the ageing process.

In view of a progressive reduction of the amount of free water in cells, the equilibrium thermodynamics of highly diluted solutions fail for realistic time scales and conditions, and non-equilibrium behaviour occurs. Using Slade's 'fringed micelle' structural model [6], we can expect that over time the cross-links would increase and the plasticization reduced.

On the other hand, it is known that in biological materials cross-linking or extensive hydrogen bonding are responsible for their low solubility in water at pH ca. 7. Also, that such materials are far more soluble at alkaline pH, in the presence of polyols or by conjugation with glucose or xylose. Moreover, in an earlier study [11], we observed that coolness is also an important factor which favours breaking or labilization of cross-links and subsequent solubilization.

In conclusion, the above data led to a justification of the use of cooling and sugar (or polyols) to help minimize cellular ageing, and to generally improve biomaterial survival.

Acknowledgements

The authors thank N. Chebib-Abuchala (technician) and S. López-Hernández (analyst physician) for valuable laboratory assistance.

References

[1] G.M. Mrevlishvili, P.L. Privalov, in Kayushin (Ed,), Water in Biological Systems, Consult Bureau, New York, 1969, pp. 63–67.
[2] C.H. Cho, S. Singh, G.W. Robinson, Faraday Discussions 103 (1996) 19.
[3] H. Susi, J. Sampugna, J.W. Hampson, J.S. Ard, Biochemistry 18 (1979) 297.
[4] M.H. Pineri, M. Escoubes, G. Roche, Biopolymers 17 (1978) 2799.
[5] C.F. Hazlewood, T.F. Egan, H.E. Rorschach, P. Läuger, L. Packer, V. Vasilescu (Eds.), Water and Ions in Biological Systems, Life Sciences, Birkhäuser Verlag Basel, Vol. 1, 1988 pp. 367–371.
[6] L. Slade, H. Levine, Adv. Exp. Med. Biol. 302 (1991) 29.
[7] M. Gavish, J.-L. Wang, M. Eisenstein, M. Lahav, L. Leiserowitz, Science 256 (1992) 815.
[8] E.C. LaCasse, Y.A. Lefebvre, J. Steroid. Biochem. Mol. Biol. 40 (1991) 279.
[9] A. Simionescu, D. Simionescu, R. Deac, J. Biomed. Mater. Res. 25 (1991) 1495.
[10] K. Nishinari, M. Watase, P.A. Williams, G.O. Phillips, Adv. Exp. Med. Biol. 302 (1991) 235.
[11] F.J. Martín-Gil, J.A. Leal, B. Gómez-Miranda, J. Martín-Gil, A. Prieto, M.C. Ramos-Sánchez, Thermochim. Acta 211 (1992) 241.
[12] M. Bonnet, J. Kopp, J.P. Renou, Water and Ions in Biomolecular Systems, Advances in Life Sciences, Birkhäuser Verlag Basel, 1990, pp. 157–164.
[13] M.L. Antonelli, M. Luciani, L. Silvestroni, Thermochim. Acta 180 (1991) 107.
[14] M.C. Ramos-Sánchez, A. Orduña-Domingo, A. Rodríguez-Torres, F.J. Martín-Gil, J. Martín-Gil, Thermochim. Acta 215 (1993) 227.